Synthesis and Structural Studies of S_P and R_P Diastereomers of Deoxyxylothymidyl-3′-*O*-acetylthymidyl (3′,5′)-*O*-(2-Cyanoethyl)phosphorothioate in Solution and in the Solid State

Marek J. Potrzebowski,*[d] Xian-Bin Yang,[a] Konrad Misiura,[a] Wieslaw R. Majzner,[b] Michal W. Wieczorek,[c] Slawomir Kaźmierski,[a] Sebastian Olejniczak,[a] and Wojciech J. Stec[a]

Keywords: Deoxyxylo dinucleotide / Pseudorotation / ^{1}H and ^{13}C NMR / ^{31}P CP/MAS / X-ray

The synthesis and full assignment of the molecular structure of the diastereomers of deoxyxylothymidyl-3′-*O*-acetylthymidyl (3′,5′)-*O*-(2-cyanoethyl)phosphorothioate (**1**) in the liquid phase based on ^{1}H, ^{13}C, 1D and 2D homo- and heteronuclear PFG (Pulse Field Gradient) NMR spectroscopic experiments are reported. The pseudorotation parameters of deoxyribose and deoxyxylose were analyzed by means of the PSEUROT program. The absolute configuration R_P and S_P of the phosphorus centers was deduced from ^{1}H ROESY experiment. The ^{31}P CP/MAS technique was used to establish the ratio between the amorphous and crystalline phases, and to test the progress of crystallization. The differences in the ^{31}P δ_{ii} principal elements of the chemical shift tensor, in particular the δ_{33} parameter, for crystalline and amorphous phases were calculated. Finally, the X-ray data for the S_P diastereomer are reported. The influence of weak C–H···S hydrogen bonding on the molecular packing of both R_p-**1** and S_P-**1**, and the significance of this type of intermolecular interaction for phosphorothioate systems is discussed.

Introduction

The utility of NMR spectroscopy for nucleic acid structure determination has long been recognized.[1] There is a number of studies showing the application of multi-dimensional NMR spectroscopic techniques to the structure elucidation of nucleotides in the liquid phase.[2] In contrast, the literature regarding the NMR spectroscopic studies of nucleotides in the solid state is not as extensive.[3−5] In this paper, we report the synthesis, the solution- and solid-state NMR spectroscopic studies, as well as the X-ray analysis of R_P- and S_P-deoxyxylothymidyl-3′-*O*-acetylthymidyl (3′,5′)-*O*-2-(cyanoethyl)phosphorothioate (R_P-**1** and S_P-**1**) containing β-D sugars.[6] Although an early interest in the chemistry of xylonucleosides was kindled by hopes of their use as intermediates in the synthesis of oligonucleotides,[7,8] most efforts were paid to their use in the synthesis of new therapeutics, such as AZT.[9] 3′-*O*-Activated xylonucleosides, if used as the substrates for oligo(nucleoside phosphorothioate)s synthesis, have shown limited application owing to the low nucleophilicity of phosphorothioate ions towards the secondary 3′-carbon atom and to the elimination process competing with the substitution.[10] Oligonucleotides containing incorporated 2′-deoxyxylonucleosides were first prepared by Shabarova,[11] and independently by Seela et al.[12] Both groups of researchers emphasized lower affinity of oligonucleotides containing incorporated 2′-deoxyxylonucleosides towards complementary DNA or RNA,[13] but their enhanced stability against nucleases. However, to our best knowledge, no detailed structural studies on oligodeoxyxylonucleotides have been reported. This paper shows the power of a multi-technique approach in the structure elucidation of the stereoisomers of dinucleotide analogues in both the liquid and solid phases. Those assignments are crucial for the unambiguous determination of the absolute configuration of deoxyxylonucleoside 3′,5′-phosphorothioates incorporated in long-chain oligonucleotides.[6]

[a] Polish Academy of Sciences, Center of Molecular and Macromolecular Studies,
Sienkiewicza 112, 90-363 Lódz, Poland
[b] Technical University, Institute of Technical Biochemistry,
Stefanowskiego 4/10, 90-924 Lódz, Poland
[c] Technical University, Institute of General Food Chemistry,
Stefanowskiego 4/10, 90-924 Lódz, Poland
[d] Center for Molecular and Macromolecular Studies, Polish Academy of Sciences
Sienkiewicza 112, 90-362 Lódz, Poland
Fax: (internat.) + 48-42/684-7126
E-mail: marekpot@bilbo.cbmm.lodz.pl

Results and Discussion

Synthesis

Diastereomers of **1** were synthesized by using the phosphoramidite method,[14] as depicted in Scheme 1.

Condensation of 5′-*O*-trityldeoxyxylothymidine 3′-*O*-(2-cyanoethyl)-*N,N*-diisopropylphosphoramidite (**2**) with 3′-*O*-acetylthymidine (**3**) in the presence of 1-*H*-tetrazole was performed in a solution of acetonitrile. The intermediate *O*-(2-cyanoethyl)phosphite **4** was not isolated, but treated with elemental sulfur resulting in the formation of fully protected dimer **5** as a mixture of two diastereomers in a ratio of 56:44 (^{31}P NMR determination). The crude diastereo-

  1434−193X/01/0408−1491 $ 17.50+.50/0

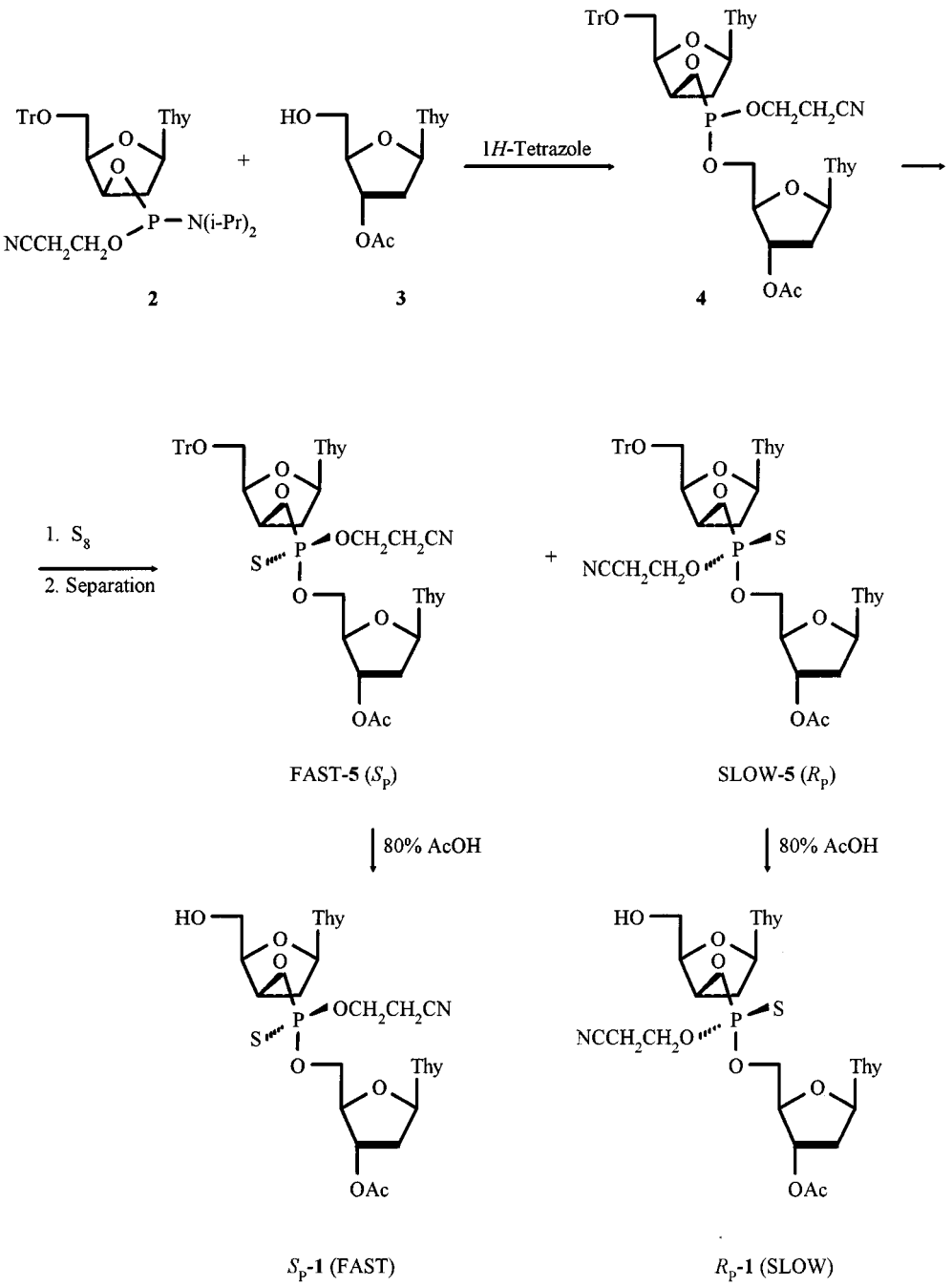

Scheme 1

mers were separated and purified by column chromatography through silica gel column. Thus, *fast*-eluted (FAST-**5**) and *slow*-eluted (SLOW-**5**) diastereomers were isolated in 37% and 23% yields, respectively. The diastereomeric purity of FAST-**5** and SLOW-**5** was confirmed by means of ^{31}P NMR spectroscopy. Each diastereomer of FAST-**5** and SLOW-**5** was deprotected by treatment with 80% acetic acid to provide FAST-**1** and SLOW-**1**, respectively. In our preliminary studies, we tentatively assigned the S_P configuration to FAST-**1** and the R_P configuration to SLOW-**1**, by means of enzymatic assays on fully deprotected dimer diastereomers.[6] The results of NMR spectroscopic and X-ray investigations presented in this paper fully proved the correctness of earlier enzymatic assignments.

^{1}H, ^{13}C NMR Studies in Solution

In this project we were attracted by the prospect of analyzing the conformation of pentose rings and elucidating the absolute configuration of the phosphorothioyl residue of S_P-**1** and R_P-**1**. For this purpose, NMR spectroscopy seemed to be the method of choice. In addition to one-dimensional ^{1}H and ^{13}C NMR spectra, several two-dimensional experiments were carried out in order to obtain the complete assignment of proton and carbon chemical shifts,

and to unambiguously elucidate the structure of S_P-**1** and R_P-**1**. In some experiments, we have taken advantage of the Pulse Field Gradient (PFG) system in order to reduce the time of measurement and to improve the quality of the spectra (e.g. reduction of T_1 noise). The ^{1}H and ^{13}C NMR chemical shifts, as well as proton-proton *J* coupling constants established by means of ^{1}H-^{1}H PFG COSY, ^{1}H-^{13}C PFG HMQC, and ^{1}H-^{13}C PFG HMBC experiments for S_P-**1** and R_P-**1** are given in Table 1. The atom-numbering system for both diastereomers of **1** is shown in Scheme 2. The accuracy of δ_{iso} and *J* assignments was confirmed by comparing experimental and theoretical spectra obtained by means of the WINDAISY program.[15]

Table 1. ^{1}H - and ^{13}C NMR spectral data

a) ^{1}H NMR chemical shifts (ppm) of furanose rings for diastereomers of deoxy*xylo*thymidine-3'-O-acetylthymidyl(3',5')-O-2cyanoethylphosphorothioate at 25°C

	S_P-*1*		R_P-*1*	
	Deoxy*xylo*se	Deoxyribose	Deoxy*xylo*se	Deoxyribose
H1'	6,13	6,16	6,12	6,20
H2'	2,19	2,33	2,24	2,37
H2"	2,79	2,26	2,78	2,29
H3'	5,10	5,16	5,09	5,22
H4'	4,04	4,12	4,04	4,31
H5'	3,70	4,21	3,69	4,18
H5"		4,24		4,20

b) J(H,H) coupling constants (Hz) of furanose rings for diastereomers of deoxyxylothymidine-3'-O-acetylthymidyl(3',5')-O-2-cyanoethylphosphorothioate at 25° C

	S_P-*1*		R_P-*1*	
	Deoxy*xylo*se	Deoxyribose	Deoxy*xylo*se	Deoxyribose
H1'-H2'	2,90	8,12	2,78	8,78
H1'-H2"	8,20	5,9	8,44	6,11
H2'-H2"	-15,60	-14,00	-15,3	-14,42
H2'-H3'	1,30	7,30	1,15	7,15
H2"-H3'	5,780	2,98	5,80	2,89
H3'-H4'	2,88	3,02	3,10	3,07
H4'-H5'	5,49	5,05	5,49	5,00
H4'-H5"		0,82		0,82
H5'-H5"	-5,78	-11,69	-5,77	-11,64

c) ^{13}C chemical shifts (ppm) for diastereomers of deoxyxylothymidine-3'-O-acetylthymidyl(3',5')-O-2-cyanoethylphosphorothioate.

	S_P-*1*		R_P-*1*	
	Deoxy*xylo*se	Deoxyribose	Deoxy*xylo*se	Deoxyribose
C1	83,06	84,11	83,04	84,03
C2	38,99	35,48	39,04	35,53
C3	63,36	67,55	63,23	67,73
C4	81,45	78,01	81,46	77,99
C5	58,85	73,52	58,94	73,53
C6	18,85		18,84	
C7	20,70		20,74	
C8	135,60; 135,47		135,49	
C9	110,08; 109,41		110,10; 109,40	
C10	163,64		163,60	
C11	150,35		150,38	
C12	118,06		117,99	
C13	170,01		170,03	

Conformation of different pentose rings in nucleosides and nucleotides including, deoxyribose and xylose, was discussed in detail by Leeuw and Altona.[16] The relationship between vicinal coupling constants and pseudorotation parameters (phase angle *P* and puckering amplitude Φ_m) is known.[17] Comparing the data for S_P-**1** and R_P-**1** with

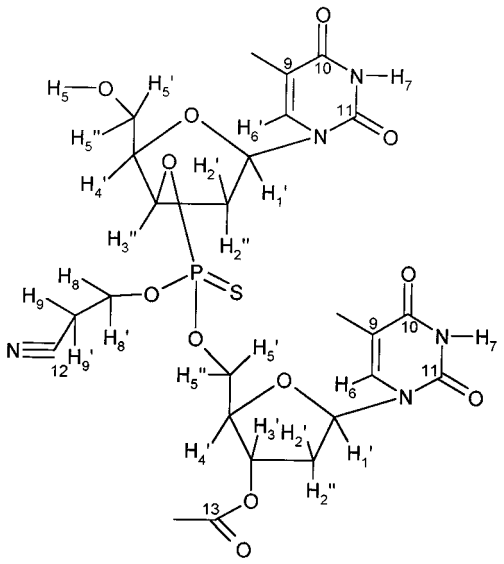

Scheme 2

those published in the literature, we can conclude that for both diastereomers, the deoxyribose rings adopt an *S*-type conformation (phase angle *ca* 180°), while deoxyxyloses adopt an *N*-type conformation (*P ca* 40°). The accurate pseudorotational parameters which best fit the experimental data can be found with the computer program PSEUROT.[18] The vicinal coupling constants taken from the WINDAISY simulation were used as input data. For the deoxyxylose ring, the constants in the Karplus equation were changed as shown elsewhere.[16] The standard routine was adopted in our calculations. The puckering amplitudes for *North*- and *South*-type conformers were held constant, then raised in 1° steps between 30° and 42°, whilst the phase angle and percentage populations were allowed to vary freely, until the best solution was found. Five parameters P_N, Φ_N, P_S, Φ_S and f_S (sum of f_S and f_N is equal to 1) fully characterize the conformations of the pentose rings. From our calculations, it was established that for the deoxyribose ring of S_P-**1**, the *S*-type conformer is the major component (f_S = 0.74 and P_S = 142.0; Φ_S = 36.5; P_N = 50.6, Φ_N = 33.0, RMS = 0.13) while the *N*-type conformer is the exclusive component for of deoxyxylose ring (f_N = 1 and P_N = 29.0; Φ_N = 36.0; RMS = 0.36). Very similar values were obtained for the R_P-**1** diastereomer. The *S*-type conformer is the major component of deoxyribose (f_S = 0.82 and P_S = 143.7; Φ_S = 34.0; P_N = 36.3, Φ_N = 35.5, RMS = 0.23) while the *N*-conformer is the only component of deoxyxylose (f_N = 1 and P_N = 30.2; Φ_N = 36.0; RMS = 0.28).

Important structural information was also obtained by analysis of NOE effects, which allow for direct proton-proton connectivity with distances up to 5 Å, through dipolar interactions. For intermediate-sized molecules with an approximate molecular weight of 1 kD, the NOE measurements are often hampered by the vanishing cross-relaxation rates. Since the measurement of transverse cross-relaxation (ROE) does not suffer from this problem, the ROESY experiments were performed for diastereomers S_P-**1** and R_P-**1**

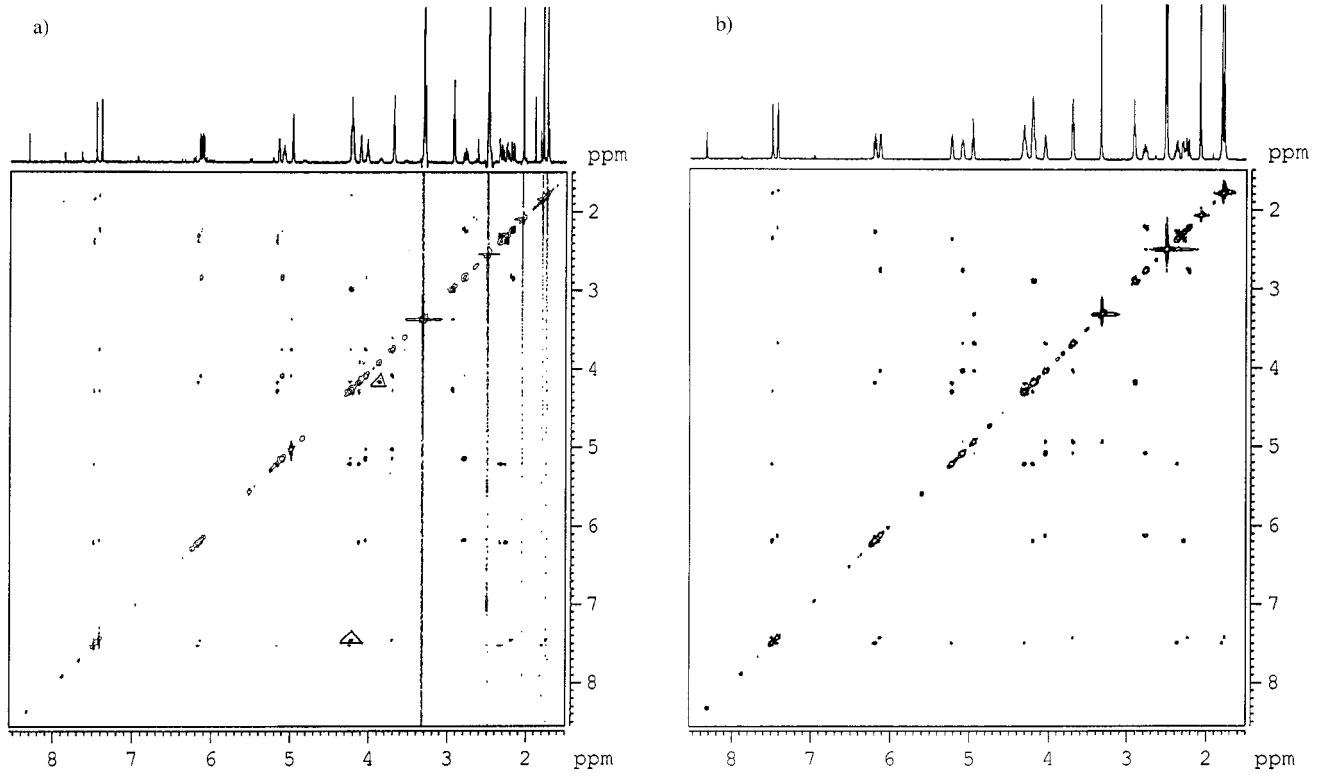

Figure 1. 500.13 MHz ^{1}H NMR ROESY spectra of a) S_P-**1** and b) R_P-**1**; both spectra recorded in [D_6]DMSO; for details see Exp. Sect.

(Figure 1, a, and 1, b, respectively). The dipolar connectivity between the protons are shown in contour plots. Employing the ROESY technique, the chemical shifts of isolated protons, *eg*. H(6) and H(6′) as well as the CH_3 groups of the thymine residues, were assigned unambiguously.

Attempts have been made to determine the absolute configuration of the phosphorothioyl residue on the basis of NOE distance constraints. The *O*-cyanoethyl group directly bonded to phosphorus was considered as a "marker" which could help in the assignment of the stereochemistry of phosphorus. Unfortunately, in the case of the S_P-**1** diastereomer, the signals for the OCH_2 group overlaps with those of the 5′ protons of deoxyribose. For R_P-**1**, the signals for the OCH_2 group overlap partially with those for the 4′ protons. However, despite these limitations, a detailed analysis of both spectra in the region of the OCH_2 resonances shows some differences. The cross-peak (inside the triangle) between the OCH_2 and the 5′ protons of deoxyxylose seen for S_P-**1** is not present in the contour plot of R_P-**1**. On the basis of molecular modeling and analysis of distances between the OCH_2 group and other centers, it is clear that only for the diastereoisomer with an *S*-configuration at phosphorus can the $OCH_2\cdots H_{5'}$ linkage of deoxyxylose be shorter than 5 Å. Another piece of evidence that supports the S_P-configuration of FAST-**1** is the cross peak between the signals for OCH_2 and H(6) of thymine (also inside the triangle). On the other hand, the lack of other cross-peaks predicted for S_P diastereoisomer does not enable us to make a final assignment of the absolute configuration at phosphorus by this approach. These ambiguities prompted us to employ other methods to investigate the absolute configuration at phosphorus in the diastereomers of **1** (vide infra).

^{31}P CP/MAS NMR Studies in the Solid State

Solid-state NMR spectroscopy is the technique that provides a link between NMR spectroscopic data in the solution or liquid phases and results obtained from single-crystal X-ray or neutron diffraction studies. A comparison of the isotropic chemical shifts and further structural results that characterize the geometry of molecules in the crystal lattice offers the possibility of drawing conclusions regarding changes in conformation and configuration, as well as the nature of the intermolecular contacts in both phases. Since SS NMR uses a powder specimen (i.e. not only one selected single crystal) this method can provide immediate information on polymorphs, solvates, inclusion complexes, etc. that may exist in the crystalline state. In this work, we have used ^{31}P CP/MAS to optimize the crystallization conditions, indicative of the presence of different crystallographic modifications, and to establish the ratio of the crystalline to amorphous phases.

The room-temperature ^{31}P CP/MAS spectra of S_P-deoxyxylothymidyl-3′-*O*-acetylthymidyl (3′,5′)-*O*-(2-cyanoethyl)phosphorothiate (S_P-**1**) crystallized from a mixture of solvents (see exp. Section) are displayed in Figure 2. The spectra show a set of spinning sidebands from the large chemical shielding anisotropy (CSA). From inspection of spectrum 2a, it is apparent that the powdered sample of S_P-**1** contains crystalline and amorphous phases in an approximate ratio of 1:10, represented by sharp and very broad

signals, respectively. As seen from spectrum 2b, the proportion of both phases is changed with improved crystallization conditions. In this work, we were interested in the analysis of the principal elements of the chemical shifts of the phosphorothioyl residue of the dinucleotide in the crystalline form, and in the correlation between δ_{ii} parameters and molecular geometry. For this purpose, a good quality spectrum of the crystalline phase was required. Taking advantage of the differences between the ^{31}P T_2 relaxation times of the crystalline and amorphous phases, the ^{31}P CP/MAS experiment was performed with a "dead time delay" of 370 μs (one over rotor period at spinning rate 2700 Hz). Figure 2 (c) presents the spectrum of sample S_P-**1** with an almost complete elimination of signals from the amorphous phase. This spectrum was further used for theoretical calculations. The principal components of the ^{31}P chemical shift tensors δ_{ii} were established from the intensities of the spinning sidebands, employing the WINMAS program, based on the Berger−Herzfeld algorithm.[19,20] The calculated values of the principal tensor elements δ_{ii} and of the shielding parameters are given in Table 2. The accuracy of the calculations was confirmed by a comparison of the experimental and theoretical spectra (Figure 3).

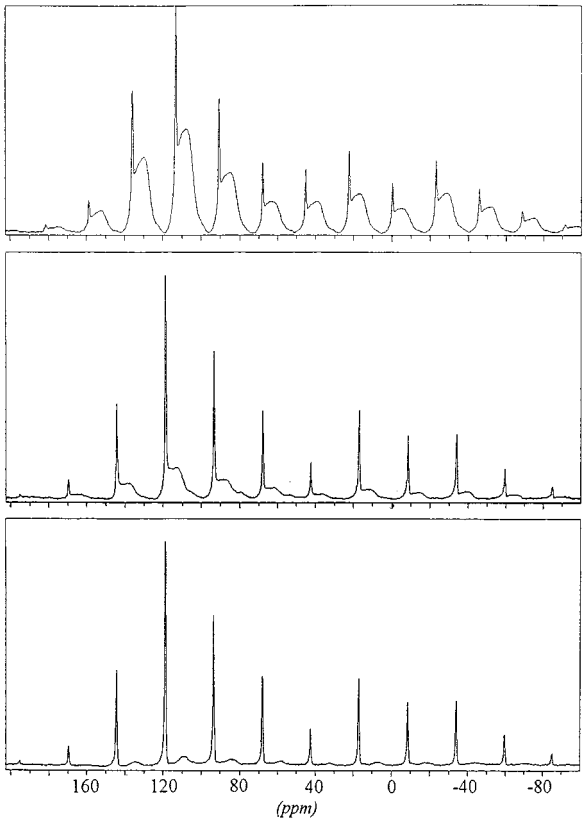

Figure 2. 121.49.46 MHz ^1H-^{31}P CP/MAS experimental spectra of S_P-**1**; the spectra have 4 K data points with 10 Hz line broadening, a contact time of 1 ms, 0.5 K scans and ν_{rot} = 2.7 kHz; a) spectrum recorded after first crystallization; b) spectrum after second crystallization with a changed proportion of solvents in the mixture; c) spectrum b recorded with a dead time delay of $1/\nu_{rot}$

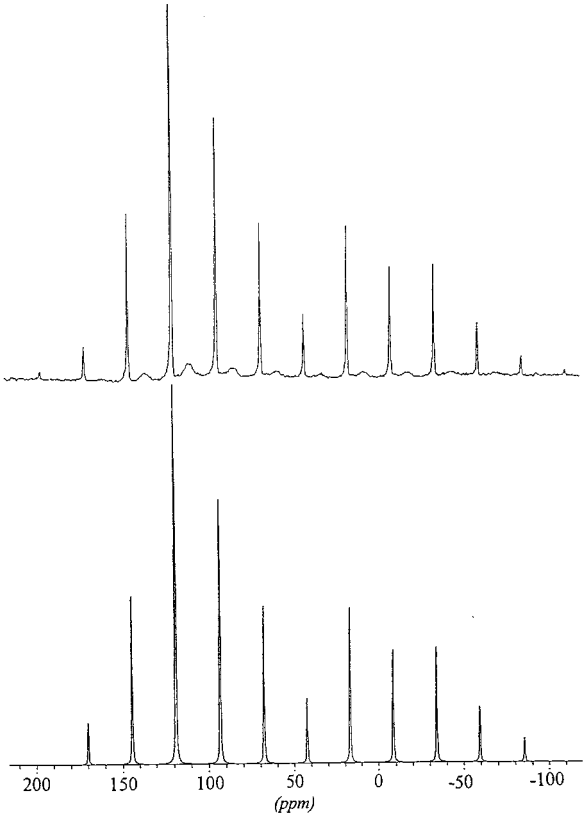

Figure 3. a) 121.49.46 MHz ^1H-^{31}P CP/MAS experimental spectrum of S_P-**1** recorded under the conditions given in Figure 2c; b) simulated spectrum calculated employing the WIN−MAS program, version 940108, Bruker−Franzen Analytik

In contrast, attempts at the crystallization of the R_P-**1** diastereomer provided only an amorphous powder. Painstaking attempts to obtain crystals of R_P-**1** failed. Thus the δ_{ii} elements were only established for the amorphous form.

Table 2. ^{31}P chemical shifts and NMR parameters for ***S*$_P$-*1*** and ***R*$_P$-*1***

Compound[a]	δ_{11}(ppm)	δ_{22}(ppm)	δ_{33}(ppm)	Δδ(ppm)	Ω(ppm)	η	κ	δ_{iso} (ppm)
S*$_P$-*1 (crystalline phase)	152	131	−81	223	233	0.14	0.81	67.8
S*$_P$-*1 (amorphous phase)	151	128	−91	230	242	0.20	0.81	62.6
R*$_P$-*1 (amorphous phase)	154	130	−92	233	246	0.16	0.85	63.6

[a] Estimated errors in δ_{11}, δ_{22}, δ_{33} and Δδ are −/+5 ppm; errors in δ_{iso} are −/+0.2 ppm. The principal components of the chemical shift tensor are defined as follows; $\delta_{11} > \delta_{22} > \delta_{33}$. The isotropic chemical shift is given by $\delta_{iso} = (\delta_{11}+\delta_{22}+\delta_{33})/3$

The experimental and theoretical spectra are shown in Figure 4, and calculated parameters are collected in Table 2. The very detailed analysis of δ_{ii} shows several structural features of S_P-**1** and R_P-**1**. It is interesting to note the considerable differences between the isotropic values of the crystalline and of the amorphous phases (≈ 5 ppm). For all modifications, only small changes in the δ_{11} and δ_{22} parameters are seen. More significant differences are established for δ_{33} and cover the range up to 10 ppm. The similar behavior of phosphorothioyl compounds, and the origin of δ_{33} changes were exhaustively discussed in a recent paper.[21] We have concluded that the effect is related to the formation of weak P=S····H−C hydrogen bonds and to the decrease in the electronic shielding of the phosphorus atom, as the phosphorothioyl group becomes more polarized during bond formation. Similar conclusions also hold for samples R_P-**1** and S_P-**1.**

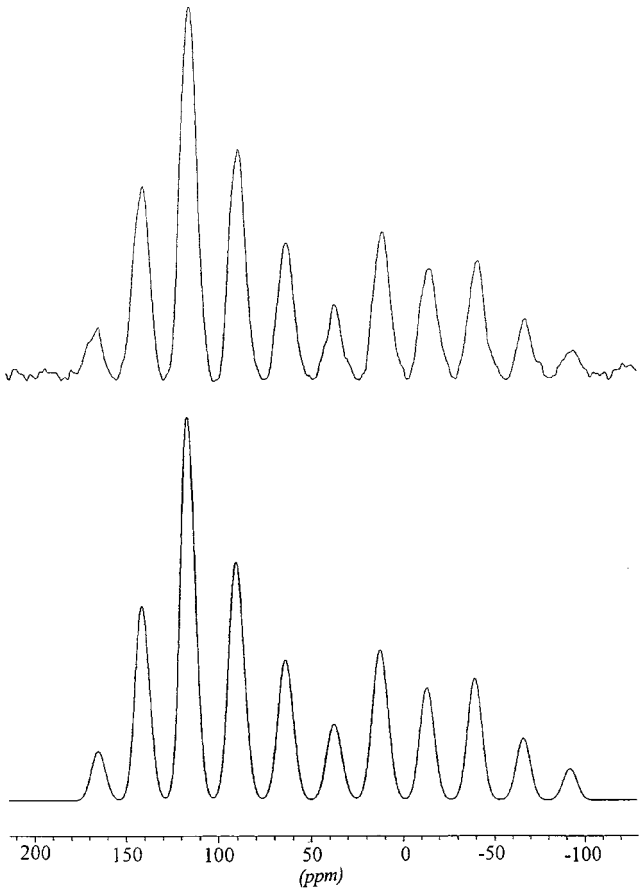

Figure 4. a) 121.49.46 MHz ^{1}H-^{31}P CP/MAS experimental spectrum of R_P-**1**; the spectrum has 4 K data points with 10 Hz line broadening, a contact time of 1 ms, 0.5 K scans and ν_{rot} = 2.7 kHz; b) simulated spectrum of R_P-**1** calculated employing the WIN-MAS program, version 940108, Bruker−Franzen Analytik

X-ray Crystallography Studies

The results obtained from solid-state NMR showing that diastereomer S_P-**1** has a tendency to form crystals prompted us to grow single crystals of suitable quality for X-ray studies. To the best of our knowledge, there are no literature reports of X-ray studies of phosphorothioate analogues of dinucleotides. Crystallographic data and experimental details for S_P-**1** are listed in Table 3. Atomic coordinates, bond lengths and angles, and torsional angles have been deposited (CCDC 147326). The thermal ellipsoid plots and the numbering schemes of S_P-**1** are shown in Figure 5.

Table 3. Crystal data and experimental details for S_P-**1**

Molecular formula		$C_{25}H_{32}N_5O_{12}PS$
Molecular mass		657.59
Crystallographic system		Monoclinic
Space group		$P2_1$
a (Å)		9.662(2)
b (Å)		14.279(5)
c (Å)		11.296(3)
β (°)		94.10(3)
V (Å^3)		1554.4(8)
Z		2
$D_{calcd.}$ (g/cm^3)		1.405
μ [cm^{-1}]		20.11
Crystal dimensions (mm)		0.2 × 0.3 × 0.8
Maximum 2θ (°)		150
Radiation, λ (Å)		Cu-K_α, 1.54184
Scan mode		ω/2θ
Scan width (°)		0.70 + 0.14·tanθ
hkl ranges:		h = −12/12
		k = −17 17
		l = 0/14
EAC correction	min.	0.9066
	max.	0.9996
	ave.	0.9643
No. of reflections:	unique	6379
refine with $I > 2\sigma(I)$		6279
observed with $I > 2\sigma(I)$		6053
No. of parameters refined		537
Largest diff. peak (eÅ^{-3})		0.344
Largest diff. hole (eÅ^{-3})		−0.158
R_{obs}		0.0355
wR_{obs}		0.0911
weighting coeff.* m/n		0.0706/0.0467
extinction coeff.** k		0.0087(5)
S_{obs}		1.063
shift/esd max		0.001
Absolute structure		S_{P1}, $R_{C1'}$, $S_{C3'}$, $R_{C4'}$, $R_{C1'a}$, $R_{C3'a}$, $R_{C4'a}$,
Flack parameter χ		−0.017(12)
R_{int}		0.0563
$T_{meas.}$		293(2)
F(000)		688

* weighting scheme $w = [\ \sigma^2(Fo^2)+(m*P)^2+n*P]^{-1}$ where $P = [\max(0,Fo^2) + 2Fc^2]/3$

** extinction method SHELXL, extinction expression $Fc^* = kFc[1 + 0.001xFc^2\lambda^3/\sin(2\theta)]^{-1/4}$

Crystallographic data (excluding structure factors) for the structure(s) reported in this paper have been deposited with the Cambridge Crystallographic Data Centre as supplementary publication no. CCDC-147326 Copies of the data can be obtained free of charge on application to CCDC, 12 Union Road, Cambridge CB2 1EZ, UK [Fax: (internat.) + 44−1223/336−033; E-mail: deposit@ccdc.cam.ac.uk].

Compound S_P-**1** crystallizes in a monoclinic system in space group $P2_1$ with the unit cell consisting of two molecules of the dinucleotide. One of the molecules is an asymmetric unit of the crystal. This observation is consistent with the ^{31}P CP/MAS experiment, in which a single line

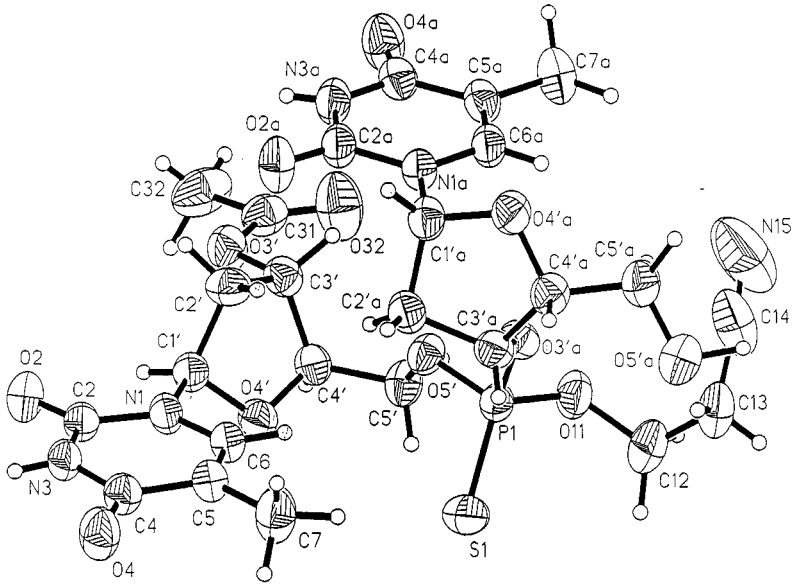

Figure 5. Molecular structure of S_P-**1** showing 50% probability displacement ellipsoids; atoms with $\sigma_{of} = 0.26$ are omitted for clarity

in the isotropic part of spectrum was detected. Molecular packing is shown in Figure 6. As seen, both molecules are bonded through intermolecular interactions; *i)* Symmetrical hydrogen bonding between thymines with participation of N(3)−H as donors and C(4)=O(4) as acceptors; and *ii)* Hydrogen bonding between the acyl block of deoxyribose and the hydroxyl group at C5 of deoxyxylose [C(31)-O(32)·····H(6′a)−C(5′a)]. The values of inter- and intramo-

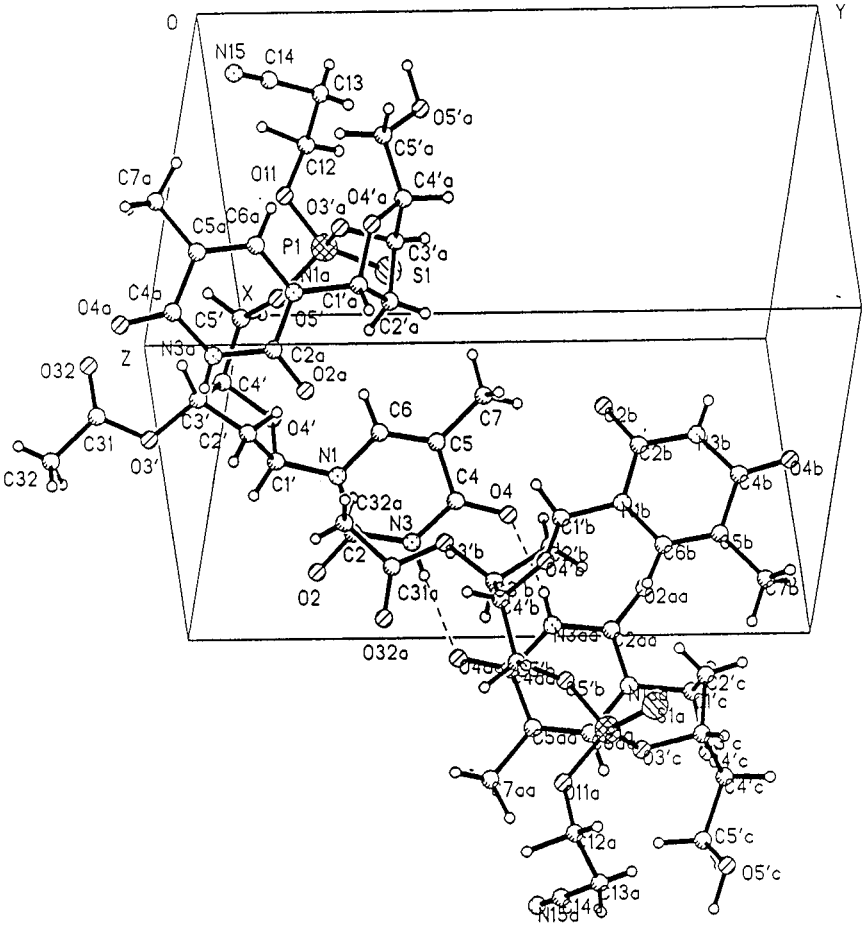

Figure 6. Crystal packing diagram for S_P-**1**; atoms with $\sigma_{of} = 0.26$ are omitted for clarity

lecular hydrogen bond lengths and bond angles presented in Table 4 are within the expected range for hydrogen bonds of this type.

Table 4. C–H···O, N–H···O and C–H···N hydrogen-bonding geometry (Å,°) for S_P-**1**

D–H···A	D–H	H···A	D···A	D–H···A
C1′–H1′···O2	0.98(2)	2.37(2)	2.765(2)	103(2)
C2′–H2′1···N1	0.90(4)	2.47(4)	2.502(3)	82(2)
C2′–H2′1···C6	0.90(4)	2.75(4)	3.157(3)	109(3)
C2′–H2′2···O4^{i}	0.96(3)	2.66(3)	3.442(3)	139(2)
C3′–H3′···O5′	1.01(3)	2.78(2)	2.932(2)	89(2)
C3′–H3′···O32	1.01(3)	2.32(3)	2.654(3)	98(2)
C5′–H5′1···O5′a^{ii}	0.94(3)	2.77(3)	3.581(3)	145(2)
N3–H3···O4a^{iii}	0.82(2)	2.04(2)	2.860(2)	178(2)
C6–H6···O4′	0.95(2)	2.42(2)	2.742(3)	99(2)
C7–H73···O4	0.98(4)	2.69(3)	2.826(3)	88(2)
C1′a–H1′a···O2a	0.94(3)	2.36(3)	2.688(2)	100(2)
C5′a–H5′a···O3′a	1.02(3)	2.53(3)	2.822(3)	96(2)
C5′a–H6′a···O32^{iv}	1.03(4)	1.71(4)	2.737(3)	173(3)
N3a–H3a···O4^{i}	0.77(3)	1.99(3)	2.747(2)	170(4)
C6a–H6a···O4′a	0.92(3)	2.41(3)	2.732(3)	101(2)
C7a–H72a···O5′a^{ii}	0.96(4)	2.52(4)	3.365(4)	147(3)
C7a–H72a···O4a	0.96(4)	2.75(4)	2.877(3)	88(3)
C7a–H73a···O4a	1.03(5)	2.70(4)	2.877(3)	89(3)
C32–H323···O2a^{i}	1.03(5)	2.70(4)	3.262(4)	115(3)
C12–H121···O4^{v}	1.18(6)	2.70(6)	3.577(4)	130(4)
C13–H131···O2^{vi}	0.87(5)	2.71(5)	3.464(4)	145(4)
C13–H132···O5′a	0.82(5)	2.68(5)	3.450(5)	157(4)
C13“–H133···O2^{vi}	1.13(10)	2.42(9)	3.419(13)	147(7)

Symmetry codes: (i) $1-x, -0.5+y, 2-z$; (ii) $-x, -0.5+y, 1-z$; (iii) $1-x, 0.5+y, 2-z$; (iv) $-x, 0.5+y, 1-z$; (v) $1-x, -0.5+y, 1-z$; (vi) $-1+x, y, -1+z$.

Our attention has been focused on possible P=S·····H–C intermolecular contacts which were suggested in the previous section. The role of CH····S hydrogen bonding and the influence of weak contacts on the molecular packing of organic crystals was very recently discussed by Borrmann et al.[22] As reported by Potrzebowski and co-workers, such interactions are not unusual for organophosphorothioyl compounds.[21] The geometric criteria for these interactions were discussed elsewhere.[21,22] The nonlinear character of such weak hydrogen bonds is proved. According to the literature, we have considered contacts within the range of the C···S distance 3.55–4.10 Å and C–H···S angles in the range 80.0–180.0°. Inspection of X-ray data given in Table 5 shows several intra- and intermolecular P=S·····H–C interactions. The most important intermolecular contacts seem to be interaction of sulfur with: *i)* The CH_3 group of thymine, *ii)* The CH_3 group of the acyl block, and *iii)* The C(4)–H of deoxyribose.

Distances and angles for deoxyribose and deoxyxylose are typical for this class of compounds. Endocyclic torsion angles and sugar thiophosphate backbone angles are shown in Table 6. A comparison of the γ_2 torsion angle for both pentoses reveals their similar absolute values and opposite signs. By definition, the *N*-type conformations are characterized by positive values of C1–C2–C3–C4-; in the *S*-type, this torsion angle has a negative value.

Table 6. a) Torsion angles of the endocyclic sugars; b) torsion angles for the sugar phosphate backbone for the ***S*$_P$*-1*** diastereomer

a)	Torsion angles			
	Definition	'Deoxyribose	Deoxyxylose	
γ_0	$C^4-O^4-C^1-C^2$	−28.6	6.3	
γ_1	$O^4-C^1-C^2-C^4$	37.7	−25.8	
γ_2	$C^1-C^2-C^3-C^4$	−32.2	33.7	
γ_3	$C^2-C^3-C^4-O^4$	16.3	−30.7	
γ_4	$C^3-C^4-O^4-C^1$	7.7	15.6	
b)		Torsion angles		
	Definition		A DNA[a]	B DNA[a]
α	$O^{3'}-P-O^{5'}-C^{5'}$	164.95	−50	−46
β	$P-O^{5'}-C^{5'}-O^{3'}$	150.22	172	−147
γ	$O^{5'}-C^{5'}-C^{4'}-C^{3'}$	47.60	41	36
δ	$C^{5'}-C^{4'}-C^{3'}-O^{3'}$	−35.70	79	157
ε	$C^{4'}-C^{3'}-O^{3'}-P$	161.09	−146	155
ξ	$C^{3'}-O^{3'}-P-O^{5'}$	106.83	−78	−96
χ_{xylo}	$O^{4'}-C^{1'}-N^1-C^2$	−159.94		
χ_{ribo}	$O^{4'}-C^{1'}-N^1-C^2$	−137.50	−154	−98

[a] Average values of the backbone torsion angles in polynucleotides (taken from ref.[2]).

Finally, the absolute *S* -configuration of the chiral phosphorus center was established by the Flack method [with $\chi = -0.017(12)$]. It should be emphasized that this result is consistent with data obtained from NMR spectroscopic

Table 5. Possible C–H···S hydrogen bonds for S_P-**1**

X–H···Y	X–H	H···Y	X···Y	(X–H···Y)	Symmetry op.
C4′–H4′ S1	0.964(24)	3.167(24)	4.083(2)	159.2(18)	$1-x,-0.5\ y, 1-z$
C5′–H5′2 S1	0.980(30)	3.091(30)	3.528(2)	108.6(19)	
C6–H6 S1	0.953(24)	3.146(24)	3.948(2)	142.8(18)	
C7–H71 S1	1.016(42)	3.021(44)	3.928(3)	149.1(33)	
C2′A–H2′A S1	0.940(30)	3.734(28)	4.047(2)	102.8(20)	
C3′A–H3′A S1	0.839(26)	2.989(25)	3.332(2)	107.0(19)	
C7A–H71A S1	0.997(33)	3.533(34)	3.672(3)	90.0(20)	$-x,-0.5+y, 1-z$
C7A–H72A S1	0.959(43)	3.455(41)	3.672(3)	95.4(26)	$-x, -0.5+y, 1-z$
C7A–H73A S1	1.034(45)	3.420(43)	3.672(3)	95.8(26)	$-x,-0.5+y, 1-z$
C32–H323 S1	1.027(47)	3.422(44)	3.864(4)	108.0(29)	$1-x, -0.5+y, 1-z$
C12–H124 S1	0.705(129)	3.096(49)	3.393(4)	109.2(67)	
C12–H122 S1	1.057(57)	3.034(52)	3.393(4)	100.7(34)	

Criteria: X–H = 0.69–1.37(Å),H···Y = 1.18–4.00 (Å), (X–H···Y) = 80.0–180.0°

studies in solution (vide supra) and with results of our earlier studies on stereodifferentiation in the enzymatic degradation of S_P- and R_P-deoxyxylothymidylthymidyl (3′,5′)phosphorothioates.[6]

Conclusions

In this work we have presented complete assignment of the structure of S_P-deoxyxylothymidyl-3′-*O*-acetylthymidyl (3′,5′)-*O*-(2-cyanoethyl)phosphorothioate (S_P-**1**) by X-ray crystallography and NMR spectroscopy in solution and in the solid state. To the best of our knowledge, it is the first report showing such results for this class of compounds. The conformational analysis in liquid and in the solid state, and the resemblance of the structures in both phases is often a matter of debate and controversy. Altona and Sundaralingman analyzed large sets of nucleotides and nucleosides, and have shown that in the case of ribose rings, the conformational preferences in the solid state are generally very similar to those established in solution.[23] It has been further concluded that intramolecular forces play a decisive role in the determination of the geometry of the ribose rings. However, this is not the case with compound S_P-**1**. The phase parameters established on the basis of the X-ray data of S_P-**1** were found to be 79.7° for the deoxyxylose ring, and 221.7° for the deoxyribose ring. The *P* values in the solid phase are considerably larger than those obtained from measurements in solution (30° for the deoxyxylose ring, $f_N = 1$, and 142° for the deoxyribose ring, $f_S = 0.74$). Instead, these results suggest that in case of **1**, the intermolecular contacts and the crystal packing effects are the dominating factors that determinate the conformation of the sugar rings in the solid state. The number of intermolecular hydrogen bonds found in the crystal lattice of S_P-**1** is shown in Table 4 and 5. The another point is the geometry of the backbone of S_P-**1**, which is characterized by several torsion angles as shown in Table 6b. This table also contains the average values of the backbone torsion angles for A DNA and for B DNA. From the analysis of this data, it is apparent that a modification of the deoxyxylose has a dramatic effect on the geometry of the whole molecule. This difference can be one of the reasons for the lower affinity of oligonucleotides containing xylo nucleosides to single-stranded DNA or RNA than that of unmodified oligonucleotides.[13]

Furthermore, comparing the NMR spectroscopic data in the solution for S_P-**1** and R_P-**1**, we found a very similar ^1H and ^{13}C data set for both diastereomers. Thus we assume that a spatial arrangement of the major segments of the dinucleotide (with the evident exception of the P=S unit) is very similar for both compounds. Finally, the intra- and intermolecular hydrogen bonds seem to play a crucial role in the crystallization process. The importance of weak P=S····H−C hydrogen bonds as one of the factors that determine the molecular packing is an open question. However, in our opinion, these weak interactions should not be neglected.

Experimental Section

Syntheses: *N,N*-Diisopropylethylamine, dichloromethane and acetonitrile were dried by distillation from calcium hydride. The progress of each reaction was monitored by TLC.

5′-*O*-Trityldeoxyxylothymidine 3′-*O*-[*N,N*-Diisopropyl-*O*-(2-cyanoethyl)phosphoramidite] (2): To a stirred solution of dry 5′-*O*-tritydeoxyxylothymidine[24] (485 mg, 1 mmol) and anhydrous *N,N*-diisopropylethylamine (700 μL, 4 mmol) in dry dichloromethane (5 mL) under an argon atmosphere at ambient temperature was added *N,N*-diisopropyl-*O*-(2-cyanoethyl)phosphoramidochloridite (335 μL, 1.5 mmol) by syringe over a period of 2 min. The obtained solution was stirred for 3.0 h. Methanol (0.1 mL) was then added, and stirring was continued for 10 min. The solvent was removed by evaporation. Ethyl acetate (200 mL) was added to the residue and the solution was washed with ice-cold aqueous sodium bicarbonate (10%, 2 × 30 mL) and brine (2 × 20 mL). The organic phase was dried with anhydrous $MgSO_4$ and evaporated to dryness. The crude product was purified by column chromatography on silica gel (silica gel: 230−400 mesh, 40 g, eluted with CH_2Cl_2/AcOEt/Et_3N, 90:8:2 v/v/v, to provide the title compound (482 mg, yield 71%): R_f 0.43 (chloroform/ethanol = 19:1, v/v). − ^{31}P NMR ($CDCl_3$) = 151.9 (49%), 148.5 (51%) (ref.[25] 151.8, 148.5 for dimethoxytrityl analogue).

S_P- and R_P-5′-*O*-Trityldeoxyxylothymidyl-3′-*O*-acetylthymidyl (3′,5′)-*O*-(2-Cyanoethyl)phosphorothioate (S_P-5 and R_P-5): To a stirred solution of **2** (431 mg, 0.5 mmol) and 1*H*-tetrazole (42 mg, 0.6 mmol) in anhydrous acetonitrile (1.0 mL) at room temperature under an argon atmosphere, was added 3′-*O*-acetylthymidine (114 mg, 0.4 mmol). Stirring was continued for 2 h, and elemental sulfur (32 mg, 1 mmol) was added. To this solution was added dichloromethane (2 mL) and stirring was continued overnight. Sulfur was removed by filtration. The solvent was removed by evaporation, and acetonitrile (50 mL) was added to the residue. The precipitated sulfur was removed by filtration, and the solvent was evaporated to dryness. The residue was dissolved in chloroform (50 mL) and the resulting solution was washed with $NaHCO_3$ (10%, 15 mL), brine (15 mL), and finally with water (2 × 15 mL). The $CHCl_3$ layer was dried over anhydrous $MgSO_4$, the solvent was evaporated to dryness. Crude product (530 mg) was purified by column chromatography on silica gel [silica gel: 230−400 mesh, 45 g, eluted with CH_2Cl_2 (100 mL), then a gradient of 0−2% methanol in chloroform] to provide the separated diastereomers as follows: (1) *Fast*-eluted diastereomer S_P-**5** (105 mg): R_f 0.49 (chloroform/ethanol, 19:1, v/v). − ^1H NMR ($CDCl_3$): δ = 1.76 (s, 3 H), 1.90 (s, 3 H), 2.07 (s, 3 H), 2.1−5.3 (m, 18 H), 6.1−6.4 (m, 2 H), 7.0−8.0 (m, 16 H), 9.89 (br. s, 1 H), 9.94 (br. s, 1 H). − δ_P ($CDCl_3$) 67.6. − MS: FAB, -ve, *m/z* = 899 [M − 1]$^-$. − $C_{44}H_{47}N_5O_{12}PS$: calcd. C 58.66, H 5.26, N 7.77; found C 58.27, H 5.62, N 7.46; (2) A mixture of diastereomers (62 mg); and (3) *Slow*-eluted diastereomer R_P-**5**, 54 mg: R_f 0.45 (chloroform, ethanol 19:1, v/v). − ^1H NMR ($CDCl_3$): δ = 1.75 (s, 3 H), 1.86 (s, 3 H), 2.10 (s, 3 H), 2.1−5.3 (m, 18 H), 6.1−6.4 (m, 2 H), 7.0−7.6 (m, 16 H), 9.56 (br. s, 1 H), 9.62 (br. s, 1 H). − ^{31}P NMR ($CDCl_3$): δ = 66.7. − MS: FAB, -ve, *m/z* = 899 [M − 1]$^-$. − $C_{44}H_{47}N_5O_{12}PS$: calcd. C 58.66, H 5.26, N 7.77; found C 58.49, H 5.52, N 7.99. The total yield of **5** was 62%.

S_P- and R_P-Deoxyxylothymidyl-3′-*O*-acetylthymidyl (3′,5′)-*O*-(2-Cyanoethyl)phosphorothioate (S_P-1 and R_P-1): *Fast*-eluted diastereomer S_P-**5** (100 mg) was treated with acetic acid (3 mL, 80%) at room temperature for 3 d. The solvent was removed by evaporation. The residue was purified by column chromatography (silica

gel, 230−400 mesh, 5.0 g: eluted with a gradient of 0−10% methanol in chloroform to provide S_P-**1** (55 mg, 72%): R_f 0.22 (chloroform, ethanol 19:1, v/v). − δ_P 67.7. − MS: FAB, +ve, m/z = 658 $[M + 1]^+$. − $C_{25}H_{32}N_5O_{12}PS$: calcd. C 45.66, H 4.90, N 10.65, S 4.88; found C 45.58, H 4.90 N 10.34 , S 4.65. S_P-**1** was crystallized from ethanol/chloroform/ hexane (1:1:1, v/v/v) to provide crystals, m.p. 189−190° C.

Starting from *slow*-eluted diastereomer R_P-**5** and using the same procedure, R_P-**1** was obtained in 68% yield: R_f 0.18 (chloroform, ethanol 19:1, v/v). − ^{31}P NMR: δ = 66.8. − $C_{25}H_{32}N_5O_{12}PS$: calcd. C 45.66, H 4.90, N 10.65, S 4.88; found C 45.36, H 4.83, N 10.30, S 4.55. Attempts to crystallize R_P-**1** from several solvents failed.

NMR Measurements in Solutions: The samples of S_P-**1** or R_P-**1** (5 mg) were dissolved in [D_6]DMSO (0.5 mL). All spectra were recorded on a Bruker Avance DRX 500 spectrometer, operating at 500.1300 MHz for ^{1}H, 125.2578 MHz for ^{13}C, and 202.46 MHz for ^{31}P. For all experiments, original Bruker pulse programs were used. The chemical shift of the DMSO signal was used as a reference (δ = 2.49 for ^{1}H and δ = 39.5 for ^{13}C). Phosphoric acid (85%) was used as an external standard for ^{31}P spectra. The spectrometer was equipped with a Pulse Field Gradient Unit (50 G/cm). The inverse broadband probe-head was used. The COSY90 spectra were obtained from 1024 experiments, each with 4 scans. The relaxation delay was 1.5 sec. The spectral width was 10 ppm (5000 Hz) in both dimensions. The data size in $F2$ was 4 K. Digital quadrature detection (DQD) was applied. Two 10 μs length z-gradient pulses, with a strength of approximately 5 G/cm each, were applied with a 1-ms delay for gradient recovery. The FID were apodized with a sine-bell function in both dimensions. Final data were zero filled twice in both dimensions and symmetrized about the diagonal. The ROESY spectra were recorded in a 2 K × 1 K ($F2$ × $F1$) data matrix. Digital quadrature detection was applied and 32 scans were accumulated in each experiment. The experiment was run in the phase-sensitive mode with a 3650 ms cw pulse for ROESY spin lock. The spectral width was 4500 Hz (9 ppm) in both dimensions. Data were processed with a sine bell shaped apodization function in both directions and TPPI in $F1$. No zero filling was applied. The PFG-HMQC spectra were acquired in a 1 K × 4 K [$F1$(^{13}C) × $F2$(^{1} H)] data matrix. Three 1 ms length z-gradient pulses, with strengths of approximately 25 G/cm, 15 G/cm, and 20 G/cm, in sequence were applied with 1 ms delay for gradient recovery. The spectral width was 4000 Hz (8 ppm) in $F2$ (^{1} H) and 25 kHz (200 ppm) in $F1$ (^{13}C). A Garp decoupling sequence was employed. Final data were processed with a sine function in $F1$ and qsine in the $F2$ dimension. The PFG-HMBC experiment was acquired in 0.5 K × 4 K ($F1$ × $F2$) data matrix and 8 scans for each experiment. Three 1-ms length z-gradient pulses, strength of about 25 G/cm, 15 G/cm and 20 G/cm, in sequence were applied with 50 μs delay for gradient recovery. Final data were processed with sine-bell and qsine-bell functions in $F1$ and $F2$ dimensions respectively.

NMR Measurements in the Solid State: Cross-polarization magic angle spinning solid-state ^{31}P NMR spectra were recorded on a Bruker 300 MSL instrument with high-power proton decoupling at 121.46 MHz for ^{31}P. The ^{31}P CP/MAS NMR spectra were recorded in the presence of high-power proton decoupling. Powder samples of S_P-**1** and R_P-**1** were placed in a cylindrical rotor and spun at 2.0−4.5 kHz. The field strength for ^{1}H decoupling was 1.05 mT, a contact time of 5ms, a repetition of 6s and a spectral width of 50 kHz were used, and 8 K data points represented the FID. Spectra were accumulated 500 times, and gave a reasonable signal-to-noise ratio. ^{31}P chemical shifts were calibrated indirectly through bis(dineopentoxyphosphorothioyl) disulfide set at 84.0 ppm. The principal elements of the ^{31}P chemical shift tensor and shielding parameters were calculated employing the WINMAS program. The details describing the method and accuracy of calculations are discussed elsewhere in detail.[19,20]

X-ray Analysis: The crystal and molecular structure of S_P-**1** was determined using data collected at room temperature on a CAD4 diffractometer with graphite monochromated Cu-K_α radiation.[26] The compound crystallizes in a monoclinic system, in the space group $P2_1$, with the unit cell consisting of two molecules. The lattice constants were refined by a least-squares fit of 25 reflections in the θ range 19.01°−28.87°. The decline in the intensity of three control reflections (3, −5, 4; 1, −7, −2; −3, −4, 1) was 1.7% during 94.0 h of exposure time. An empirical absorption correction was applied by the use of the ψ-scan method (EAC program).[27] A total of 6279 reflections with $I \geq 2\sigma(I)$ were used to solve the structure by direct methods and to refine it by full-matrix least-squares using F^2. Hydrogen atoms at the disordered −O−CH2−CH2−C≡N group with gof = 0.26(2) were placed geometrically, and allowed to ride on the preceding C atom with a C−H distance free to refine and fixed thermal parameters equal to 1.3 times the equivalent isotropic thermal parameter of the parent-atom. All other hydrogen atoms were found on a difference-Fourier map and refined isotropically. Anisotropic thermal parameters were applied for all non-hydrogen atoms. The final refinement converged to R = 0.0355 for 6053 reflections with $I \geq 2\sigma(I)$. The absolute configuration at the chiral atoms were established as S_{P1}, $R_{C1'}$, $S_{C3'}$, $R_{C4'}$, $R_{C1'a}$, $R_{C3'a}$, $R_{C4'a}$. The absolute structure was determined by the Flack method,[27] with the resulting χ = −0.017(12).

Data Collection and Cell Refinement: Absorption correction: *EAC*.[28] Structure solution: *SHELXS*-86.[29] Structure refinement: *SHELXL*-93.[30]

Acknowledgments

This project was financially assisted by the State Committee for Scientific Research, grants 3 T09A 026 19 (to M.J.P.) and 4 P05F 006 17 (to W.J.S.).

[1] K. Wüthrich, *NMR of Proteins and Nucleic Acids*, Wiley, New York, **1986**.
[2] S. S. Wijmega, M. M. W. Mooren, C. W. Hilbers, chapter *NMR of Nucleic Acids; From Spectrum to Structure* in *NMR of Macromolecules, A Practical Approach*, (Ed.: G. C. K. Roberts), IRL Press, Oxford, **1993**, pp. 217−289.
[3] H. Shindo in *Phosphorus-31 NMR*: *Principles and Applications*, Ed. D. G. Gorenstein, Academic Press, New York, **1984**, pp. 401−422.
[4] C. W. Hilbers, S. S. Wijmega, in *Encyclopedia of Nuclear Magnetic Resonance*, (Eds.: D. M. Grant, R. K. Harris), Wiley, Chichester, **1996**, pp. 3346−3359.
[5] P. M. Macdonald, M. J. Damba, K. Ganeshan, R. Braich, S. V. Zabarylo, *Nucleic Acid Res.* **1996**, *24*, 2868−2876 and references cited therein.
[6] X.-B. Yang, K. Misiura, M. Sochacki, W. J. Stec, *Bioorg. Med. Chem. Lett.* **1997**, *7*, 2651−2656.
[7] J. Zemlicka, J. Smrt, *Tetrahedron Lett.* **1964**, *5*, 2081−2086;
[8] Y. Mizuno, T. Sasaki, *Tetrahedron Lett.* **1965**, *6*, 4579−4584.
[9] H. Mitsuya, K. J. Weinhold, P. A. Furman, M.H. StClair, S.N. Lehrman, R.C. Gallo, D. Bolognesi, D. W. Barry, S. Broder, *Proc. Natl. Acad. Sci. USA* **1985**, *82*, 7096−7010.
[10] X.-B. Yang, K. Misiura, W. J. Stec, *Heteroatom Chem.* **1999**, *10*, 91−104.
[11] N. I. Sokolova, N. G. Dolinnaya, N. F. Krynetskaya, Z. A. Shabarova, *Nucleosides Nucleotides* **1990**, *9*, 515−531.

[12] H. Rosemeyer, M. Krecmerova, F. Seela, *Helv. Chim. Acta* **1991**, *74*, 2054−2067.
[13] H. Rosemeyer, F. Seela, *Nucleosides Nucleotides* **1995**, *14*, 1041−1045.
[14] M. H. Caruthers, *Science* **1985**, *230*, 281−285.
[15] WINDAISY program, version 940108, Bruker−Franzen Analytik, Bremen, **1994**.
[16] F. A. A. M. de Leeuw, C. Altona, *J. Chem. Soc., Perkin Trans. II* **1982**, 375−384.
[17] F. A. A. M. de Leeuw, C. Altona, *J. Comput. Chem.* **1983**, *4*, 438−441.
[18] C. A. G. Haasnoot, F. A. A. M. de Leeuw, H. P. M. de Leeuw, C. Altona, *Org. Magn. Reson.* **1981**, *15*, 43−52.
[19] G. Jeschke, G. Grossmann, *J. Magn. Reson.* **1993**, *A103*, 323−328.
[20] WIN-MAS program (1994) version 940108, Bruker−Franzen Analytik, Bremen
[21] M. J. Potrzebowski, M. Michalska, A. E. Koziol, S. Kazmierski, T. Lis, J. Pluskowski, W. Ciesielski, *J. Org. Chem.***1998**, *63*, 4209−4217
[22] H. Borrmann, I. Persson, M. Sandström, C. M. V. Stälhandske, *J. Chem. Soc., Perkin Trans. 2* **2000**, 393−402.
[23] C. Altona, M. Sundaralingam, *J. Am. Chem. Soc.* **1972**, *94*, 8205−8212.
[24] J. J. Fox, N. C. Miller, *J. Org. Chem.* **1963**, *28*, 936−941.
[25] H. Rosenmeyer, F. Seela, *Helv. Chim. Acta* **1991**, *74*, 749−760.
[26] B. A. Frenz, *Enraf−Nonius Structure Determination Package*; *SDP User's Guide.* Version of 17 December 1986. Enraf−Nonius, Delft, The Netherlands **1986**.
[27] H. D. Flack, *Acta Cryst.* **1983**, *A39*, 876−881.
[28] A. C. T. North, D. C. Phillips, F. S. Mathews, *Acta Cryst.* **1968**, *A24*, 351−359.
[29] G. M. Sheldrick, *Acta. Cryst.* **1990**, *A46*, 467−473.
[30] G. M. Sheldrick, *J. Appl. Cryst.* **1993**.

Received July 31, 2000
[O00403]